Role of Surface Tension in Microrobot Penetration in Membranes

1st Md Mahmudur Rahman
Dept. of Mechanical Engineering
Georgia Southern University
Statesboro, GA, USA
m.rahman@louisville.edu

2nd Tanmay Garudadri
Dept. of Mechanical Engineering
University of Delaware
Newark, DE, USA
garudadri.tanmay17@gmail.com

3rd Sambeeta Das
Dept. of Mechanical Engineering
University of Delaware
Newark, DE, USA
samdas@udel.edu
(Corresponding author)

***Abstract*—cell-membrane fusion using microrobots can be a useful technique for delivering bioactive compounds to cellular systems. The role of membrane curvature and lipid ordering in the cell membrane penetration process is well known. However, once the fusion into the cell membrane is already initiated, the fluid dynamics of microrobot penetration based on tension difference of the microrobot solution and membrane curvature at the fusion pore has not been explored yet. Here, we demonstrate how surface tension difference among merging interfaces plays role in microrobot droplet penetration into a liquid bath, mimicking cell membrane fusion. The maximum penetration of a microrobot droplet into a liquid bath depends on the positive difference of surface tension between the droplet and liquid bath, longitudinal curvature of the bridge region, and the size of the droplet.**

***Index Terms*—Microrobots, Biological Cell Manipulation, Surface Tension, Colloidal Transport**

I. Introduction

Micromachines such as microrobots have been envisioned as a potential advancement in precision medicine or drug delivery. Due to the demand of biocompatible design in facilitating microrobot movement in biological fluids and ability to interface and interact with the surrounding environment, microrobots [1], [2] show enormous potentials. One such example could be to deliver magnetic microrobots (which are essentially magnetic particles that may carry necessary cargo molecules on its surface [3]) to appropriate cell or tissue locations. To ensure efficient delivery of cargo molecules from cell-like microrobots at the destination, cell-membrane fusion can be a useful technique. Cell membrane fusion [4]–[6] is one of the important and ubiquitous processes in cellular biology. However little is known about the mechanism of cell membrane penetration mechanism. Therefore, unfolding the mystery of fusion pore expansion mechanism or membrane penetration mechanism is an important step for efficient drug/cargo delivery using microrobots.

The role of membrane curvature and lipid ordering in the viral membrane fusion process has been discussed before [7]. However, once the fusion pore is already initiated, the fluid dynamics of microrobot (or cellular contents) penetration based on tension difference of the merging membranes and membrane curvature at the fusion pore has not been explored yet. In nature, vesicles with increased internal pressure, when work as closed systems, resemble tiny water droplets with Laplace pressure. Drop-bath coalescence and cell membrane fusion process, below a critical temperature [8], can share the same hydrodynamic process once both continuous phases are connected by a liquid bridge (pore). Hydrodynamics of drop coalescence has been studied for a long time from theoretical [9], [10] and experimental perspective (some of them are listed in [11]. The main focus of those studies involves early and later dynamics, pressure-driven flow, viscous resistance, internal flow [12], the role of outer fluids [13], viscous vs inertial dominance [14] etc. Drop impact on a thin film [15]–[18] and subsequent rebounding, partial and complete coalescence [19], coalescence cascade [20] has also been studied extensively where the role of film thickness, surface tension, impact inertia and liquid viscosity has been investigated.

Here, we studied penetration dynamics of microrobot solution into a liquid bath, upon penetration, thus mimicking a cell membrane penetration event by microrobots. Surface tension, viscosity, size of the robot solution, bridge (pore) curvature are the key parameters that play role in the penetration process. We demonstrated that the tension difference among merging interfaces defines the fate of the penetration depth of the microrobot solution in a liquid bath. In the following discussion, we show a theoretical argument on how pressure difference from both continuous fluids to the merging interface at the onset of penetration can be determined.

First, we consider the coalescence of the same-sized mirror droplets. Coalescence is governed by forming a liquid bridge between merging droplets. Once there is a bridge formation, Laplace pressure from the bulk drop is released due to the pressure difference between a bulk drop and the bridge region. A detailed physical process has been explained previously (in Section B.1, [11]). Driving pressure from the bulk drop to the bridge region, when outer fluid is air, is expressed by the following equation,

$$\Delta \mathrm{P}_d = \frac{\sigma_d}{R}\left[2 + \frac{2}{A\bar{r}^2} - \left(\frac{2}{A} + 1\right)\frac{1}{\bar{r}}\right] - \frac{1}{2}\rho U^2 \qquad (1)$$

where, σ_d, R, A, ρ, U, and $\bar{r}$ represent surface tension of the microrobot droplet, radius of the microrobot droplet, longitudinal curvature factor at the bridge region, density of the microrobot droplet, bridge propagation rate in the radial

direction and dimensionless bridge radius (normalized by drop radius) respectively. Parameter A is defined as actual longitudinal radius at the bridge region (red circle in Figure S1 in the Supporting Information) divided by the radius of a fitting sphere between two merging droplets (green circle in Figure S1) before coalescence at the bridge surface. Therefore, the more widening curvature (higher radius) at the bridge region will contribute to higher A value. Considering that the liquid drop invokes bridge curvature during coalescence with a liquid bath, driving pressure from liquid bath to the bridge region can be approximated[1] by the following equation,

$$\Delta \mathrm{P}_b = \frac{\sigma_b}{R}\left[\frac{2}{A\bar{r}^2} - \left(\frac{2}{A}+1\right)\frac{1}{\bar{r}}\right] - \frac{1}{2}\rho U^2 \tag{2}$$

From Equation 1 and 2, we can get net pressure difference at the very early stage ($\bar{r} << 1$) of coalescence which determines drop penetration or rebounding, as expressed by the following equation,

$$\Delta \mathrm{P}_d - \Delta \mathrm{P}_b = \frac{2}{AR\bar{r}^2}\left(\sigma_d - \sigma_b\right) \tag{3}$$

From the early stage of coalescence (Equation 3), drop penetration (complete coalescence [19] can happen due to the positive difference of surface tension between the drop and the bath. However, partial rebounding (coalescence cascade [20]) can happen due to the negative difference of surface tension between the drop and the bath. Driving pressure on the merging interface at the onset of coalescence also depends on the longitudinal curvature factor (A) and the size of the droplet (R). Therefore, at the onset of coalescence, pressure difference from the drop side to the bath side is the function of the positive surface tension difference between the drop and the bath, the radius of the bridge curvature at the longitudinal direction and the drop radius. While we can keep the drop size same, increasing surface tension difference leads to decreasing in longitudinal bridge curvature (radius of the curvature increases) [21], [22], which contributes to larger A, as shown in Figure S1. Therefore, a critical surface tension difference is expected to contribute to maximum penetration if drop size remains constant. To validate the theoretical argument, we conducted experiments to observe different penetration depths while changing surface tension difference between the microrobot droplet and the bath. We also conducted experiment to observe initial penetration velocity for different sized drops while surface tension difference between merging interfaces is the same.

II. Materials and Methods

Magnetic microrobots were fabricated using 500 nm carboxylate modified polystyrene microparticles. 20 nm of Nickel and 10 nm of titanium dioxide was deposited using soft lithography techniques to make the particles magnetic (due to Ni) and biocompatible (due to titanium dioxide). The microrobots were premagnetized with 1mT of magnetic field. 1.25% (v/v) of the magnetic microrobots was dissolved in DI water to generate the microrobot droplet.

To ensure complete penetration of the microrobot droplet into the liquid bath, the surface tension of the droplet (σ_d) must be higher or equal than the surface tension of the bath (σ_b). Here, we prepared the liquid bath by adding Sodium Dodecylsulfate (SDS, CH3(CH2)10CH2OSO3Na, 98% purity, bought from Eisen-Golden Laboratories, Dublin, CA, USA) in 250 mL of DI water at different concentrations (0.05 mM, 0.1 mM, 0.5 mM, and 1 mM), which lowered the surface tension below the critical micelle concentration (CMC at 8 mM [20]). In one set of experiments, surfactant solutions were mixed well with DI water and in another set of experiments the same amount of surfactant solutions, from 87.6 mM stock solutions, were added on the top surface to ensure above micelle concentration so that surface tension remains the same at the bath interface. The latter set of experiments was conducted to learn if any effects other than surface tension plays role in the observed phenomena. 2.5 µL and 1.0 µL of the liquid drop was gently touched at the bath surface using a micropipette, as shown in Figure 1. Drops were released from the micropipette tip upon coalescence with the liquid bath so that drop impact on the bath surface was minimized. Downward sinking velocity due to gravity was also very insignificant (Bond number, $Bo = \frac{\rho g R^2}{\sigma} \sim 0.1$). Microrobot solutions were washed two times with DI water using a centrifuge. We conducted experiments at 23°C and 50% relative humidity. Experiments were captured using the camera of Moto G Stylus (2021) smartphone at 60 fps.

III. Results and Discussion

A. Critical surface tension difference in maximum penetration depth

While early dynamics ($\bar{r} << 1$) of drop coalescence is universal and depends on fluid properties, later dynamics can change the fate of coalescence significantly depending on outer fluids [13] or bounded surface [12]. Here, the later dynamics is assumed identical for all experiments and we examined the role of initial dynamics on drop penetration by changing surface tension difference of merging interfaces. With increasing surface tension difference $[(\sigma_d - \sigma_b)]$, according to Equation 3, fluid pressure from liquid drop towards the bath increases at the onset of coalescence ($\bar{r} << 1$). Therefore, we can expect maximum penetration of the drop into the bath at the maximum tension difference. However, with increasing surface tension difference longitudinal curvature at the bridge region decreases (radius of curvature increases) Therefore, we can expect a critical tension difference for which maximum penetration can happen. Surface tension differences between DI water and different SDS-DI water mixers are shown in Table I, according to the study from [24].

The theoretical understanding of maximum penetration depth at critical surface tension difference was validated by

[1]The First term on the right-hand side of Equation 1 is $\frac{2\sigma_d}{R}$, which represents Laplace pressure of the bulk drop (please see section B.1. in [11]). However, in the case of a liquid bath, this term contributes to zero because there is no such pressure for a liquid bath as R is much larger compared to the drop radius. This is how Equation 2 is formulated.

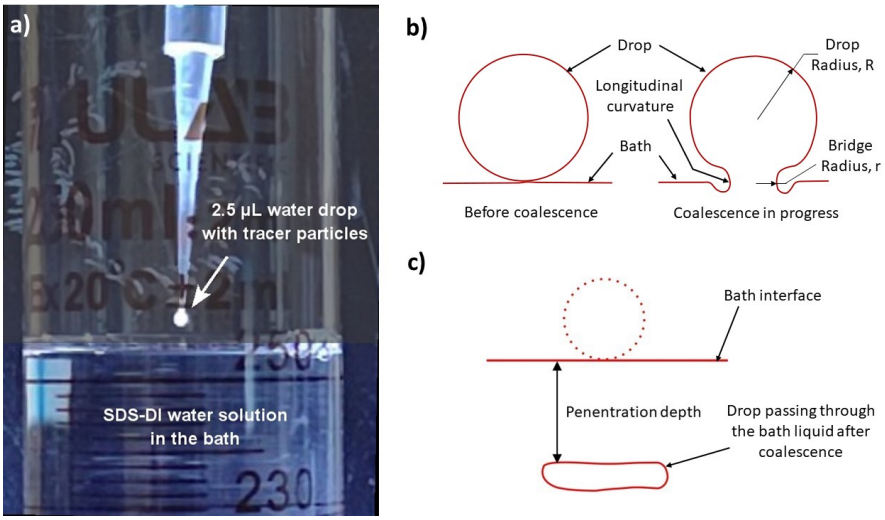

Fig. 1. a) Experimental setup for coalescence of the liquid drop and the liquid bath. 2.5 µL droplets were gently touched at the air-water interface of the liquid bath. b) Schematic diagram shows a typical coalescence process of a water drop with a liquid bath. The longitudinal curvature at the bridge region can be of wide varieties depending on surface tension differences between merging interfaces. c) After merging, liquid drop penetrates through the liquid bath. Penetration depth is measured from the bath interface to the top of the penetrated drop at a given time.

TABLE I
APPROXIMATE SURFACE TENSION DIFFERENCES AMONG MERGING INTERFACES AT 25°C. THE SURFACE TENSION OF DI WATER AT 25°C IS 72 mN/m [25].

SDS in DI water (mM)	Surface tension [24] (mN/m)	$[(\sigma_d - \sigma_b)]$ (mN/m)
0.05	-	-
0.1	60.5	11.5
0.5	44	28
1.0	33	39
3.0	25.5	46.5
$>$ CMC	35	37

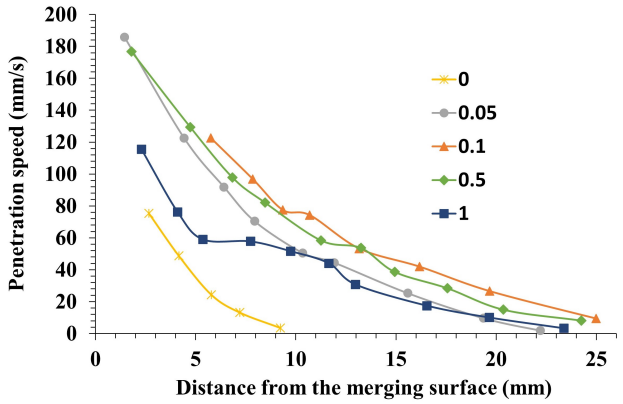

Fig. 2. (Color online) Penetration speed of a droplet with respect to its distance from the merging surface at varying surfactant concentration in the water bath (shown by the legend values). 0.1 mM SDS in DI water was found to be the critical concentration at which penetration speed was maximum.

tracking the velocity of the droplet inside the bath for each surface tension difference, which is shown in Figure 2. The water bath containing 0.1 mM SDS $[(\sigma_d - \sigma_b) = 11.5mN/m]$ maintained a higher velocity of the drop inside the bath at all distances from the bath interface, while lower velocity was observed at a higher surface tension difference (such as 1.0 mM SDS in DI water bath, $[(\sigma_d - \sigma_b) = 39mN/m]$).

It is important to note that while a certain (or critical) tension difference among merging surfaces ensures maximum penetration depth, as shown in Figure 3, further increase in tension difference lowers penetration depth but not at the same scale. For example, penetration depth at 1.0 mM SDS (10X higher surfactant concentration than the SDS concentration of 0.1 mM where penetration was maximum) was 22.58 mm while penetration depth at 0.05 mM SDS (2X lower SDS concentration than 0.1 mM) was 21.23 mm after 2.5 s from the onset of coalescence. Mixing of the microrobots to some extent was observed during coalescence for zero tension differences between merging interfaces. However, mixing was nearly absent for all other coalescence when there was tension differences among merging interfaces $[(\sigma_d - \sigma_b) > 0]$.

Bridge formation at the early stage of coalescence can be extremely minuscule where differential viscous resistance may have played role in the dynamics [11]. Therefore, to eliminate any possible role of other parameters, due to surfactant concentration differences, except surface tension in the observed behavior, the same amount of surfactant solutions (from 87 mM stock solution) were added at the top surface of the bath so that it can form micelle at different concentrations above CMC near the bath surface. Almost similar penetration depths were observed for all concentration differences (Figure S2), which is lower than the maximum penetration depth at the equilibrium solution of 0.1 mM SDS in DI water bath. Therefore, viscous resistance at the early stages were identical for all experiments which were conducted at equilibrium surface tension concentration. Note that local surface tension

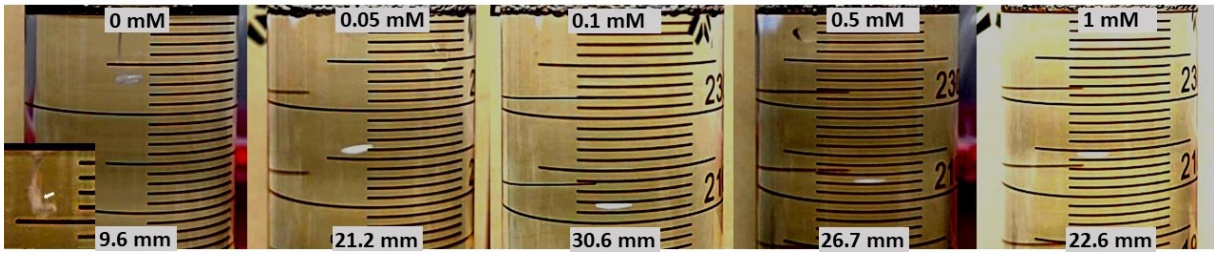

Fig. 3. Drop penetrates maximum distance when the tension difference among merging interfaces are at a critical difference. After 2.5 s from the onset of coalescence, tension difference of 11.5 mN/m between the bath (0.1 mM SDS solution in DI water) and the drop interfaces facilitated maximum penetration depth (30.6 $\pm$ 0.2 mm) of the droplet in the water bath while penetration depth is 22.6 $\pm$ 0.2 mm (lower) when tension difference is higher (39 mN/m) than the critical difference. (Inset) Trail of the microrobots from penetrated droplet was observed (shown by the white arrow) when tension difference was zero. In all other cases, mixing during coalescence was nearly absent.

difference (at the onset of coalescence) plays role in penetration dynamics as suggested by our theoretical argument. However, dynamic surface tension (changes of surface tension during coalescence) may have a role in the penetration process as well depending on how it changes evolving pressure and longitudinal curvature at the bridge region.

Here, we investigated the role of early stage of coalescence in penetration dynamics while we disregarded viscous resistance as we did not vary viscosity for different experiments. Surface tension difference plays role in widening curvature at the bridge region. The surface tension difference for viscous fluids can play role in changing later dynamics as well, such as by adding more viscous resistance through surface driven flow in the opposite direction due to Marangoni effect.

B. Smaller drop penetrates at a higher velocity at the interface

As we predict from Equation 3, the velocity of the smaller droplet at the early stage, despite higher viscous resistance during coalescence [11] due to higher Ohnesorge number ($Oh = \frac{\mu}{\sqrt{\rho R \sigma}}$), was higher than the velocity of the bigger drop, as shown in Figure 4. During flow in the bath, higher viscous resistance further slows the penetration speed for the smaller drop and hence penetration depth is lower for the smaller droplet (Figure S3).

Smaller droplets penetrating at a higher initial velocity further justifies that Equation 3 can guide penetration dynamics through useful information even though we did not account viscous resistance at the early stage of the coalescence. Further investigation is needed to understand the role of viscosity in evaluating critical surface tension difference in maximum penetration for higher viscous fluids through the modification in early and later dynamics.

IV. Conclusion

Theoretical understanding predicts that at the onset of drop merging with a liquid bath, flow drives into the bridge region from both continuous phases depending on the magnitude of their respective surface tensions which leads to complete or partial coalescence. Here, we demonstrated that the positive tension difference from a microrobot drop surface to the liquid bath surface plays role in facilitating as well as obstructing

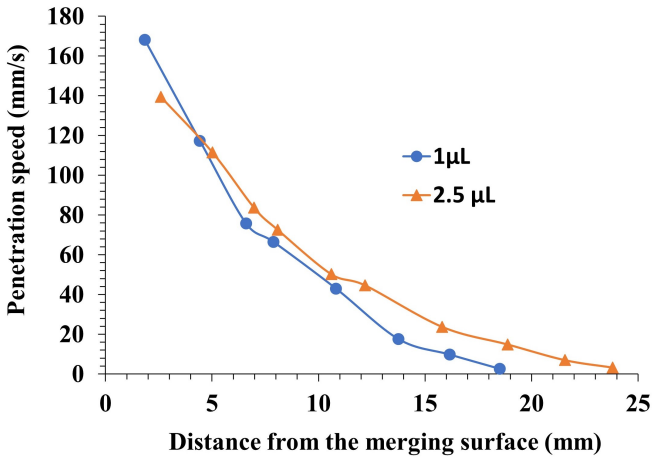

Fig. 4. (Color online) Penetration speed at the early stage of coalescence for the smaller droplet is higher than the bigger one. Both experiments were conducted at 0.1 mM SDS concentration in the DI water bath solution. SDS was added to the top surface from 87.6 mM stock solution.

flow which ends up in different microrobot penetration depths. We observed a critical surface tension difference among merging interfaces for which penetration depth is maximum. While higher surface tension difference enhances penetration, wider curvature (higher radius) at the longitudinal direction in the bridge region as a result of higher surface tension difference, works as an obstruction in the flow at the early stage of coalescence. Our work can explain how efficiently a microrobot can penetrate the cell or tissue depending on membrane tension difference during the cell-membrane fusion process once fusion pore is initiated. Hydrodynamics of cell membrane fusion can be important specially at a lower temperature than the body temperature. Below a critical temperature, tension builds up in the vesicle membrane [8] which can contribute to efficient biomolecule transfer while zero tension difference may lead to lipid and biomolecule mixing upon fusion. The research can be useful in diverse field of studies such as virus-cell fusion process, presynaptic neurotransmitter release mechanism, inject printing where drops are the building blocks, and in various microfluidic applications. The penetration dynamics

can be optimized as desired by changing surface properties (such as by changing membrane contents, adding surfactant or by modulating temperature) or by changing size of the drop.

AUTHOR'S CONTRIBUTION

MR contributed to the conception of the work, writing of the manuscript, and the interpretation of the results. Both MR and TG conducted the experiments. SD secured funding, supervised the project, and reviewed the manuscript.

CONFLICT OF INTEREST

The authors declare that the research was conducted in the absence of any commercial or financial relationships that could be construed as a potential conflict of interest.

SUPPORTING INFORMATION

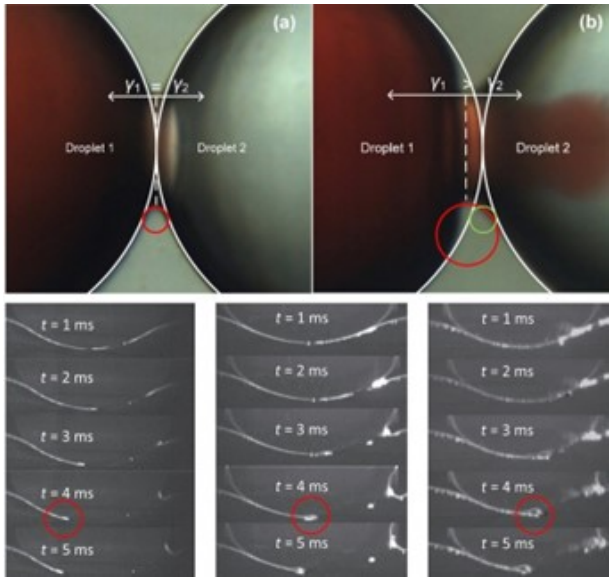

Fig. S1. (Top row) Lowering surface tension in one drop led to wider curvature (higher radius) in the longitudinal direction of the bridge region which contributed to larger A in Equation 3 (main text). Here, A represents the ratio of the red circle (actual curvature) to the green circle (fitting circle between two drops at the bridge surface. It contributed to roughly more than 2X larger A in (b) compared to in (a). The white circle indicates droplet position before merging while the red circle denotes curvature in the longitudinal direction when coalescence is in progress. The symbol denotes the surface tension of each droplet. The image is adapted with permission from X. Luo et al. "Electrocoalescence of two drops with different surfactant concentrations suspended in oil.", The Journal of Physical Chemistry C 122, 22615 (2018). Copyright 2018 American Chemical Society. (Bottom row) The longitudinal curvature of the bridge region decreases significantly (radius increases) with lowering the surface tension of the merging interface (higher surfactant concentration on the interface due to higher surface age), marked by the red circle. The image is adapted from Dong et al. "Laser induced fluorescence studies on the distribution of surfactants during drop/interface coalescence." Physics of Fluids 31.1 (2019): 012106. Copyright 2019 AIP Publishing.

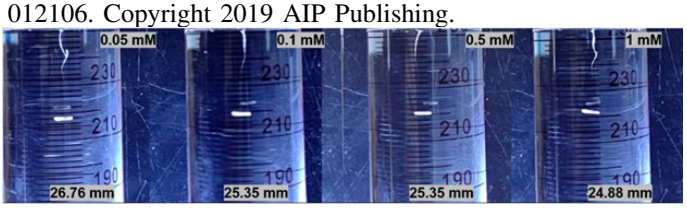

Fig. S2. After spreading the required amount of SDS solution from 87.6 mM stock solution on top of the 250 mL DI water bath, we observed almost the same penetration depth of the droplet in the water bath, after 2.5 s from the onset of coalescence, for all concentration distribution. SDS stock solution was concentrated mostly on the upper part of the water bath which made surface tension almost equal for all the cases with different micelle concentrations.

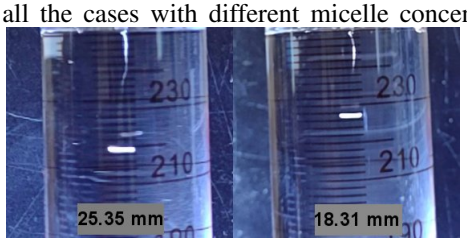

Fig. S3. After 2.5 s from the onset of coalescence, the bigger droplet (2.5μL, left) penetrated a larger distance (25.35 mm) compared to the smaller droplet (1μL, right).

REFERENCES

[1] B. Esteban-Fernández de Ávila, W. Gao, E. Karshalev, L. Zhang, J. Wang, Cell-like micromotors. Accounts of Chemical Research 51, 1901-1910 (2018).

[2] R. H. Fang, A. V. Kroll, W. Gao, L. Zhang, Cell membrane coating nanotechnology. Advanced Materials 30, 1706759 (2018).

[3] Das, Sambeeta and Hunter, Elizabeth E and DeLateur, Nicholas A and Steager, Edward B and Weiss, Ron and Kumar, Vijay. (2018). Controlled delivery of signaling molecules using magnetic microrobots. 2018 international conference on manipulation, automation and robotics at small scales (MARSS) (pp.1-5). IEEE.

[4] R. Jahn, T. C. Südhof, Membrane fusion and exocytosis. Annual review of biochemistry 68, 863-911 (1999).

[5] L. V. Chernomordik, M. M. Kozlov, Protein-lipid interplay in fusion and fission of biological membranes. Annual review of biochemistry 72, 175-207 (2003).

[6] L. Chernomordik, A. Chanturiya, J. Green, J. Zimmerberg, The hemifusion intermediate and its conversion to complete fusion: regulation by membrane composition. Biophysical journal 69, 922-929 (1995).

[7] L. G. M. Basso, E. F. Vicente, E. Crusca Jr, E. M. Cilli, A. J. Costa-Filho, SARS-CoV fusion peptides induce membrane surface ordering and curvature. Scientific reports 6, 1–19 (2016).

[8] R. Kwok, E. Evans, Thermoelasticity of large lecithin bilayer vesicles. Biophysical journal 35, 637–652 (1981).

[9] R. W. Hopper, Coalescence of two equal cylinders: exact results for creeping viscous plane flow driven by capillarity. Journal of the American Ceramic Society 67, C–262 (1984).

[10] J. Eggers, J. R. Lister, H. A. Stone, Coalescence of liquid drops. Journal of Fluid Mechanics 401, 293–310 (1999).

[11] C. R. Anthony, M. T. Harris, O. A. Basaran, Initial regime of drop coalescence. Physical Review Fluids 5, 033608 (2020).

[12] M. M. Rahman, W. Lee, A. Iyer, S. J. Williams, Viscous resistance in drop coalescence. Physics of Fluids 31, 012104 (2019).

[13] J. D. Paulsen, R. Carmigniani, A. Kannan, J. C. Burton, S. R. Nagel, Coalescence of bubbles and drops in an outer fluid. Nature communications 5, 1–7 (2014).

[14] J. D. Paulsen, J. C. Burton, S. R. Nagel, Viscous to inertial crossover in liquid drop coalescence. Physical Review Letters 106, 114501 (2011).

[15] S. Lakshman, W. Tewes, K. Harth, J. H. Snoeijer, D. Lohse, Deformation and relaxation of viscous thin films under bouncing drops. Journal of Fluid Mechanics 920 (2021).
[16] X. Tang, A. Saha, C. K. Law, C. Sun, Bouncing-to-merging transition in drop impact on liquid film: Role of liquid viscosity. Langmuir 34, 2654–2662 (2018).
[17] T. Tran, H. de Maleprade, C. Sun, D. Lohse, Air entrainment during impact of droplets on liquid surfaces. Journal of Fluid Mechanics 726 (2013).
[18] S. T. Thoroddsen, M. J. Thoraval, K. Takehara, T. G. Etoh, Microbubble morphologies following drop impacts onto a pool surface. Journal of fluid mechanics 708, 469–479 (2012).
[19] F. Blanchette, L. Messio, J. W. Bush, The influence of surface tension gradients on drop coalescence. Physics of fluids 21, 072107 (2009).
[20] S. Shim, H. A. Stone, Damped coalescence cascade of liquid drops. Physical Review Fluids 2, 044001 (2017).
[21] X. Luo et al., Electrocoalescence of two drops with different surfactant concentrations suspended in oil. The Journal of Physical Chemistry C 122, 22615-22621 (2018).
[22] T. Dong, W. H. Weheliye, P. Angeli, Laser induced fluorescence studies on the distribution of surfactants during drop/interface coalescence. Physics of Fluids 31, 012106 (2019).
[23] M. M. Rahman, S. J. Williams, Membrane tension may define the deadliest virus infection. Colloid and Interface Science Communications 40, 100338 (2021).
[24] S.-Y. Lin, Y.-Y. Lin, E.-M. Chen, C.-T. Hsu, C.-C. Kwan, A study of the equilibrium surface tension and the critical micelle concentration of mixed surfactant solutions. Langmuir 15, 4370-4376 (1999).
[25] Heller, W., Cheng, M.-H., and Greene, B. W. (1966). Surface tension measurements by means of the “microcone tensiometer”. Journal of colloid and interface science 22, 179–194